COMPUTING DYNAMIC POWER LIMITS

8.1: Introduction

- One final look at the course roadmap shows that our journey is nearly complete.

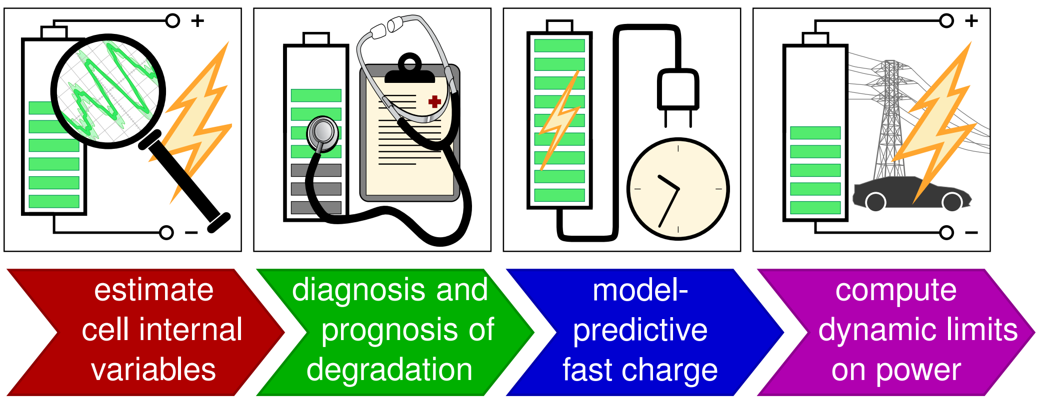

  - In the previous chapter, we applied MPC to obtain an optimizing fast-charge profile guided by underlying electrochemical limits.
  - In this chapter, we extend the fast-charge concept to develop a physics-based approach to battery power-limits estimation.
- Definitions for state of energy (SOE) and state of power (SOP) are not hard-and-fast, and some ambiguity persists in their application.
  - In this chapter we attempt to bring some clarity to this discussion and illustrate how to use a predictive framework with physics-based models to generate online estimates of SOP.
- Similar to SOC, both SOE and SOP (in their various definitions) are not directly measurable with sensors, and thus can only be estimated from available externally defined quantities.

- ECE5720 outlined a method for SOP estimation using ECMs and provided general background on SOP methods.
  - Here, we build on that earlier development to construct a comprehensive framework for understanding SOP and then introduce a physics-based application.

Energy and power

- ECE5720 introduced the idea that careful management of energy flow into—and out of—a battery is of paramount concern to a BMS.
  - Recall: energy is the ability of the battery to do work, and is a total quantity typically measured in Wh or kWh for vehicle applications.
  - Remaining total energy defines a fuel gauge equivalent for a BEV and relates to the vehicle's available driving range.
  - A state of energy measure is often used to capture this quantity.
    - In general practice, however, SOC is normally used instead as it trends in the same sense as SOE and is easier to estimate.
  - Although they are fundamentally related, the relationship that links SOC with SOE is not straightforward.
  - Mathematically, SOC is obtained via the integral of applied current, whereas SOE is computed using the integral of the product of current and terminal voltage, which complicates its evaluation.[1]
- It is important to note that total energy is to be distinguished from available energy, in that the latter takes into account the manner in which the energy is removed from the battery.

[1] Total energy is related to SOC as $E = \left[\int_{z_{\min}}^{z} \mathrm{OCV}(\xi)\,\mathrm{d}\xi\right] \times Q$ for a single cell. It is more complicated to compute for a battery pack (see ECE5720) and is not equivalent to available energy.

- We mention this here because it provides a direct connection to the idea behind state of power.
- Whereas energy content defines useable range, it is the rate at which this energy is transported which ultimately influences a vehicle's performance.
- The time-rate-of change of energy is what we call power, and it is on this topic we will focus the remainder of this chapter.

■ Since energy within a battery is stored as charge, power thus relates to the movement of charge into and out of a battery cell, and this dynamic is governed by its time-dependent current-voltage behavior.

- When we speak of a high-power cell, for example, we generally mean a battery where current can be drawn off (or inserted) at a high rate, which when multiplied by its instantaneous voltage, delivers a correspondingly high value of power.
- The converse is true for the case where transport of charge is inhibited (by increased internal resistance, for example).

■ Estimating available power on charge and discharge enables a vehicle controller to manage battery utilization wisely for efficient operation of BEVs and HEVs.

- Accurate estimation of SOP over a future time horizon assists with planning for acceleration and regenerative braking requirements, among other operational demands.
- The following sections outline a practical definition of SOP and present a physics-based model-predictive method for its computation.

8.2: State of power

- SOP is generally defined to mean how much power—on charge or discharge—can be sustained over a specified future time interval.[2]
- The term lends itself to a variety of interpretations in the literature.
  - In some cases, it is used to refer to an instantaneous *peak* power level available at a given moment in time.[3]
  - More generally it is used in a predictive sense over a future time horizon, as in the definition introduced above.
- The premise is that we wish to supply an upcoming load demand (e.g., accelerate, climb a hill, or accept charge from regenerative braking) and must inform the application controller of what it can safely expect from the battery at its present state.
  - This is a critical element in HEV energy management and is equally important in BEVs to ensure the battery is operated safely.
- Thus in our development we shall define SOP as the maximum *constant* power level that can be supplied by or introduced to a battery cell over a defined power horizon, which we term ΔT.
- We shall next introduce a visual representation of SOP to facilitate our understanding of these terms.

Voltage-current plot

- It is insightful to generate simplified SOP estimates based on standard current profiles such as constant-current (CC), constant-voltage (CV), or constant-current-constant voltage (CCCV).

[2] ECE5720 employed the term *power limits* for this quantity; here we synonymously adopt the widely used term state of power to describe the same metric.
[3] This is also sometimes called “state of function (SOF)”.

- It is important to note that these cases violate the constant-power (CP) ideal, and SOP estimates made using these will generally depart from the true value.
- This is easy to see as follows:
  - A nonzero constant applied current brings about a change in voltage due to the fact that charge is either entering or leaving the cell electrodes and the SOC-OCV relationship is monotonic.
  - Similarly, maintaining constant voltage requires a changing value of applied current (or zero current).
  - Therefore, it is not possible to achieve constant power while holding either the voltage or the applied current constant; in fact, both must change simultaneously.
  - Thus, any SOP calculations based on the simplified assumption of either constant current or voltage are necessarily inaccurate.
- To illustrate the impact of these assumptions and provide a useful framework for understanding general SOP behavior, we employ a simple voltage-current (VI) plot, where current is displayed on the abscissa and voltage on the ordinate axis.
- For visual simplicity, only positive values of current are used; charge or discharge cases will be evident by context.
- Each point on the plot represents an instantaneous power value computed as the product $P(t) = v(t) \times i(t)$.
- Contours of constant power are drawn for reference.

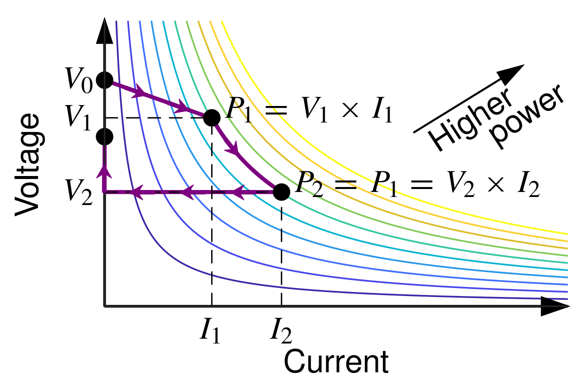

- The purple trace indicates the trajectory of instantaneous power for a cell discharge event starting at an equilibrium voltage, V_0.
- Sudden application of discharge current I_1 brings about an instantaneous drop in cell voltage to V_1 due to ohmic resistance; the absolute value of the slope is equal to the ohmic resistance value, R_0.
- The corresponding instantaneous power level is $P_1 = V_1 \times I_1$.
- In this example, the discharge current is controlled so as to maintain a constant power level—denoted by alignment with the constant power contour traversed between points $P_1 = V_1 \times I_1$ and $P_2 = V_2 \times I_2$.

Constant-current-constant-voltage discharge

- We first demonstrate a long duration discharge power trajectory for a battery cell where maximum and minimum limits are imposed on both current and voltage and a CCCV discharge strategy is employed.
- Starting from an initial SOC $z(0)$, maximum instantaneous power is achieved immediately at the maximum applied current level $I_{\max}$ (we assume the cell is initially at equilibrium with $i(0) = 0$).
- Assuming we reach $I_{\max}$ without encountering any other limit, then in order to sustain this power level into the future we need to maintain a constant voltage at the applied current $I_{\max}$.
- But since OCV is monotonically decreasing with discharge, voltage must drop for a sustained current level.
- So, our trajectory moves downward on the VI plot and instantaneous power continuously decreases until reaching lower voltage limit $V_{\min}$.
- Another possibility: we reach SOC bound $z_{\min}$ before reaching $V_{\min}$.

- In this case, $i(t)$ will drop to zero and the voltage will relax to equilibrium.
- The VI plot shows simulated instantaneous discharge power behavior of a modified NMC30 cell (R_c was increased for illustrative purposes).

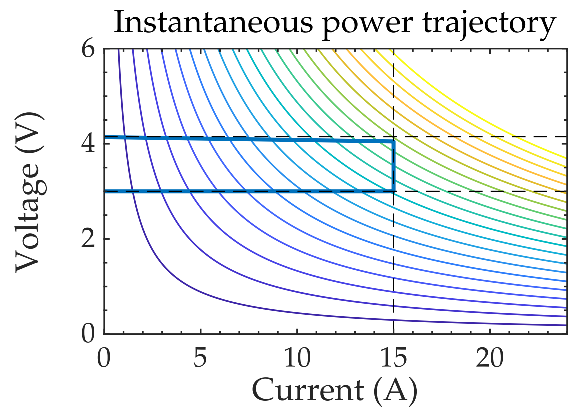

- Starting at initial SOC $z(0) = 1$ and corresponding OCV of $4.15\,\mathrm{V}$, a maximum rated discharge current of $15\,\mathrm{A}$ is continuously applied until the minimum voltage limit of $3.0\,\mathrm{V}$ is reached.
- Current then reduces to maintain the lower voltage limit as described.
- For this example, instantaneous maximum power $P_{\max} = 60.8$ W is achieved immediately upon application of maximum current, after which instantaneous power continuously decreases to $P_{\text{inst}} = 44.1$ W when the lower voltage bound is reached.
- This value is simply $P = V_{\min} \times I_{\max}$. Upon reaching $V_{\min}$, current continuously decreases to zero proportionate with P_{inst}.
- The figures below show show current, voltage, and instantaneous power plots corresponding to this CCCV discharge.

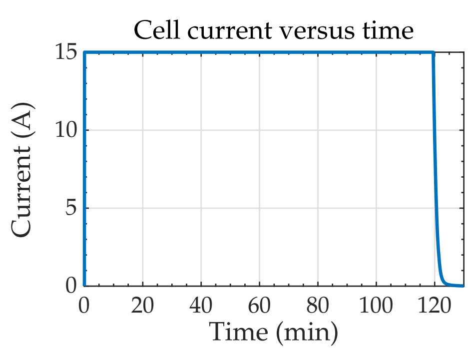

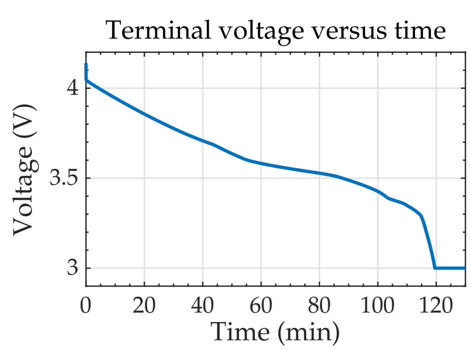

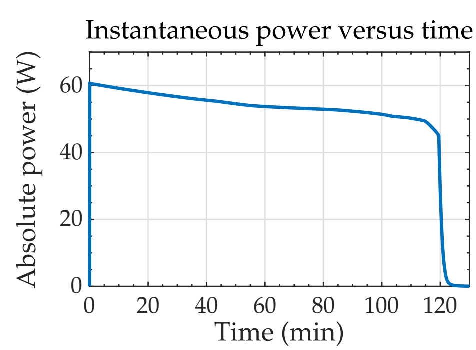

- We note here that constant discharge current results in decreasing voltage and a correspondingly decreasing power level, implying that the CC assumption cannot bring about a sustained constant power level and that power limit estimates derived with this assumption will exhibit conservatism, especially at longer power horizons.

Constant-power-constant-voltage discharge

- We next demonstrate a discharge trajectory where again maximum and minimum limits are imposed on both current and voltage but now a constant-power-constant voltage (CPCV) strategy is employed.
- The figure depicts the corresponding VI portrait where it is easy to see that the CPCV strategy follows a constant power contour until reaching $V_{\min}$.
- Then, the CV current is applied.

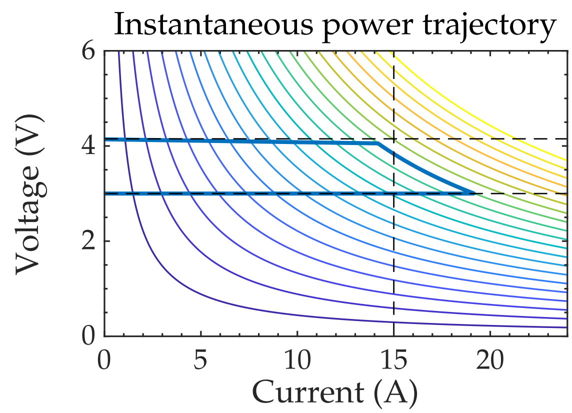

- Note: the maximum constant power derived SOP value is $57.5\,\text{W}$.
- The figures below show current, voltage, and instantaneous power plots corresponding to the CPCV discharge case presented above.

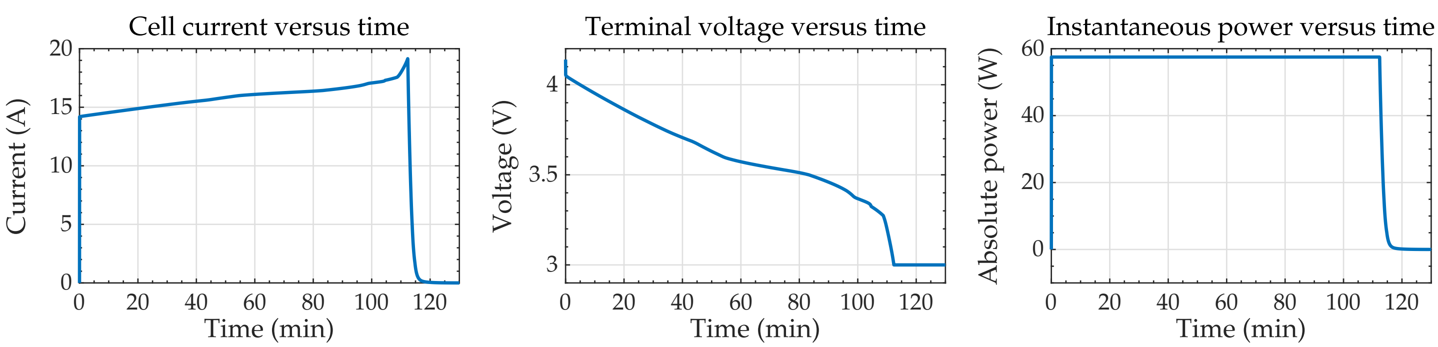

- It is clear from this simulation that constant power generally requires both current and voltage to change in opposition to one another, thus reaffirming that assumptions of CC (or CV) made to simplify SOP calculation will normally result in conservative SOP estimates.

- The preceding examples suggest a surprisingly simple calculation for the maximum constant discharge power over a long duration power horizon (i.e., one measured in minutes), namely, $P = V_{\min} \times I_{\max}$.
- Let's explore this situation a bit further.
  - We've assumed for our examples that the only relevant limits are imposed on cell voltage and discharge current.
  - Furthermore, we assumed we could achieve the maximum current level without encountering any other limits.
  - Note, however, that if the current limit is high enough, the initial cell voltage low enough, and/or the cell's internal resistance is high enough, then $V_{\min}$ may be encountered well before reaching $I_{\max}$.
  - We can picture this as a steepening of the initial slope in the VI trajectory (which is proportional to cell resistance) causing the plot to intersect the $V_{\min}$ bound prior to reaching the $I_{\max}$ boundary.
  - This causes an immediate curtailment of instantaneous power which cannot be held constant without violating the voltage limit.
  - In this case, once $V_{\min}$ is reached, the current (and power) must continue to decrease to maintain the constant minimum voltage.
- In most vehicle applications we are not interested in long duration horizons, but typically consider power prediction on the order of seconds, with 10 to 20 s a commonly used range for xEVs.
- Sustaining power over a short horizon means we are generally less likely to encounter a lower voltage limit on discharge, especially at high values of initial SOC.
- In this case, we must consider the upper current limit as the bounding event for maximum sustained power.

- Turning again to the VI plot, we seek a trajectory that intersects the largest constant power contour it can follow prior to encountering the maximum current limit within that specified time interval.

- An example is shown in the figure.
- Clearly this becomes a rather complicated calculation to make and one can quickly appreciate the desire to find suitable approximations.

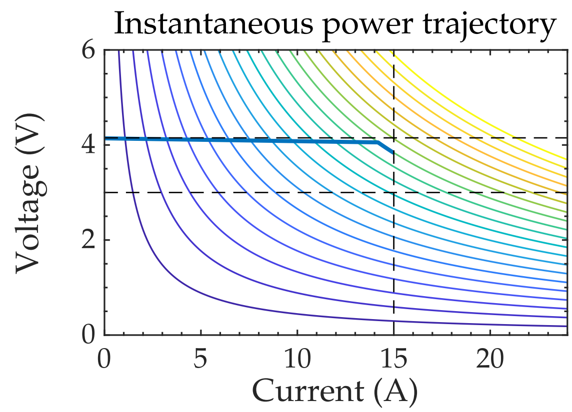

- Our discussion so far suggests that cell internal resistance will ultimately govern short-term power availability for a battery cell.
- However, we have purposely oversimplified the problem by only placing bounds on external measurable quantities cell voltage and applied current.
- In reality, the issue is far more complicated.

8.3: SOP estimation

- Practically speaking, it is not straightforward to compute SOP as defined here since it involves a constrained nonlinear optimization.
- Most authors instead resort to simpler SOP formulations, which are easier to obtain yet characterize true SOP in some less precise, but nonetheless meaningful way.
- In some applications, it may be important to predict peak power, which we define here as the maximum instantaneous value of power attainable over a future time period.
- This differers from our SOP definition; nevertheless we note here the obvious fact that the maximum constant power over ΔT approaches the maximum instantaneous power as $\Delta T \to 0$.

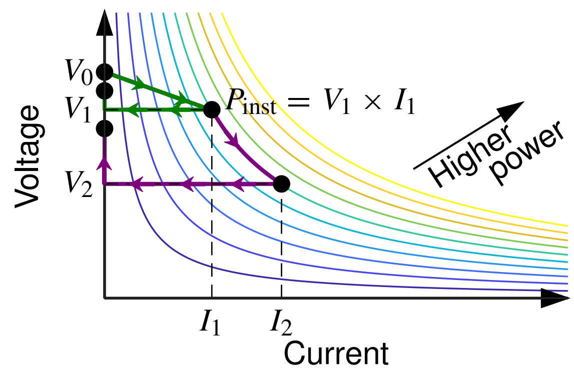

- This idea is illustrated in the figure.
- So far, we have discussed maximizing instantaneous power; but, our ultimate interest is to maximize predicted power over a time interval.
- In the following sections, we leverage this paradigm to formulate predictive power-limit estimation strategies and compare behaviors.
- SOP cannot be measured by direct sensing: thus, must be estimated from measurable information. e.g., voltage, current, temperature.
- Since the measurements themselves are considered fixed, we are left to select: (1) a mathematical model, and (2) a computational method to use to determine our SOP estimate.

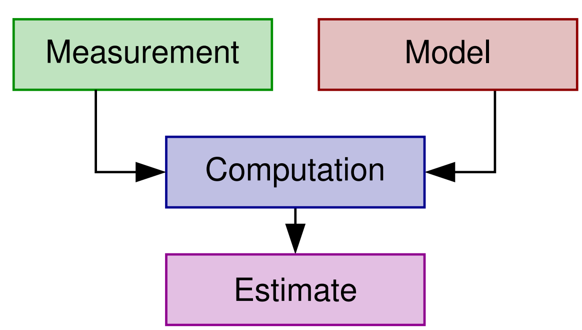

- The following development shall make use of the notation:

$v[k]$	Cell terminal voltage at time k
$z[k]$	Cell state-of-charge at time k
$P[k]$	Cell instantaneous power at time k
$i[k]$	Cell applied current at time k

- For ease of plotting, we shall occasionally refer to the maximum value of both charge or discharge current as the positive value $I_{\max}$.
  - i.e.,we treat the charge/discharge current as its absolute value.
- The basic idea behind the computation of dynamic power limits can then be stated as follows: Starting at time index k,
  - Compute $P_{\text{limit}}[k]$ according to the predictions of $v[k]$, $i[k]$, and internal electrochemical variables over the time interval $\{k,\ k+1, \ldots,\ k+k_{\Delta T}\}$, where $k_{\Delta T}$ is the number of discrete-time time steps in real-time interval ΔT seconds.
- In general, a predictive estimate of available power is preferred over an instantaneous estimate to allow for load-schedule optimization over a near-term horizon.
- In short, we wish to know how much power can be sustained over a specified time into the future, termed the *power horizon*, which we shall denote mathematically by ΔT.
- Since the constant power level sustained must be less than or equal to the maximum instantaneous power, the predictive estimate can be considered conservative in some sense.
- A common prediction-horizon value used by the automotive industry is $\Delta T = 10$ s; we shall use this value in subsequent calculations.

- We note further that power limits are a dynamic measure—a function of the evolving operational environment of the battery.
- Thus, power limits must be updated periodically in order to supply timely and useful load-planning information—this update rate is typically more frequently than once every ΔT.
- Hence, our computation methodology must include a prediction component that can supply needed model variables out to the length of the power horizon.
- A computation of maximum power is ultimately limited by bounds or constraints on certain cell-level quantities that may be adversely affected by the rapid movement of current.
- In this sense, the max-power problem resembles that for fast charge.
- For simplicity, we shall only consider here limits imposed on: current, voltage, and SOC; these are of course relevant for the case of ECMs.
  - Nonetheless, the concepts easily generalize to the PBM case with inclusion of hard bounds on certain electrochemical quantities.
  - We illustrate the idea of maximum power by simple example: first examining instantaneous discharge power, then charge power.
- ECE5720 introduced a very effective bisection-based method that utilized a state-space equivalent circuit model (ECM) and a polytopic[4] set of hard constraints to compute power limits.
  - We term this the “bisection method” (PL-BSM).

[4] The term *polytopic* refers to constraints that appear as a set of parallel hyperplanes in the parameter space.

- PL-BSM assumes a constant level of input current ΔT seconds into the future for its estimates; we shall review the essential elements of this method in the next section.

- While effective, we might wonder if PL-BSM is perhaps a bit too conservative in that it fails to consider the dynamic nature of the predicted response within the power prediction window.
- To that end, we shall investigate an alternative method (PL-MPC) that makes use of the full dynamic profile and compare this to PL-BSM.
- Furthermore, PL-BSM considered only empirical ECMs and relied only on voltage-based and SOC-based performance limits.
  - So again here we may wonder if a physics-based model (PBM), harboring electrochemical parameter information, might bring about a more accurate power limits estimate.
  - We'll introduce this improved PL-BSM approach in this chapter.
  - Finally, we'll combine the PBM with PL-MPC to explore the potential of computing dynamically predictive power limits governed by true electrochemical quantities.
- Before proceeding, we recall a few definitions:

DISCHARGE POWER: maximum discharge power that may be maintained constant for ΔT seconds without violating design limits.

CHARGE POWER: maximum battery charge power that may be maintained constant for ΔT seconds without violating design limits.

- We note that both quantities are based on the present battery state.
- In this chapter, we develop power limits for single cells; the methods are readily adapted to obtain pack-level estimates as per ECE5720.

8.4: Bisection method of SOP estimation

- By way of brief review, this method of SOP estimation relies on a general state-space model of battery dynamics,

$$\boldsymbol{x}[k+1] = \boldsymbol{f}(\boldsymbol{x}[k],\ i[k])$$

$$v[k] = h(\boldsymbol{x}[k],\ i[k]),$$

to compute a predicted battery state at a fixed time index $k + k_{\Delta T}$.

- Assuming a constant current is applied throughout the duration of the power horizon (i.e., from time index k to $k + k_{\Delta T}$), the method computes the appropriate constant current value ($i_{\max}^{\text{dis,volt}}[k]$ and $i_{\min}^{\text{chg,volt}}[k]$) that brings the predicted terminal voltage to a prescribed limit ($V_{\min}$ or $V_{\max}$) ΔT seconds in the future.

- This is accomplished by seeking the $i[k]$ values that bring about:

$$V_{\min} = h(\boldsymbol{x}[k + k_{\Delta T}], i[k]), \qquad V_{\max} = h(\boldsymbol{x}[k + k_{\Delta T}], i[k]),$$

$$0 = h(\boldsymbol{x}[k + k_{\Delta T}], i[k]) - V_{\min} \qquad 0 = h(\boldsymbol{x}[k + k_{\Delta T}], i[k]) - V_{\max}$$

for $i_{\max}^{\text{dis,volt}}[k]$ and $i_{\min}^{\text{chg,volt}}[k]$, respectively.

- These equations may be solved for the limiting $i[k]$ using the bisection search algorithm.

- SOC-based limits can also be computed similarly: refer to ECE5720 Ch. 6 for additional details.

- Using this method, the products:

$$p_{\min}^{\text{chg}}[k] = i_{\min}^{\text{chg}}[k]v[k + k_{\Delta T}]$$

$$p_{\max}^{\text{dis}}[k] = i_{\max}^{\text{dis}}[k]v[k + k_{\Delta T}]$$

give the SOP estimates for charge and discharge, respectively.

8.5: Model predictive method of SOP estimation

- In ECE5720, SOP estimates were computed using ECMs together with designated limits on current, voltage, and SOC.
  - Although a carefully identified ECM can give a very accurate picture of battery cell input–output voltage (and SOC) behavior, it cannot provide useful information about internal electrochemical properties that determine the genuine boundaries of performance.
  - Consequently, ECM limits may be considered only indirect indicators of true physics-based limits, as was true for fast charge.
  - Thus, power limit estimates based solely on ECM prediction models will not, in general, be exact bounds.
- Ch. 7 applied model-predictive methods to a PBM to obtain an optimizing fast-charge profile guided by electrochemical limits.
- In the following sections, we leverage the same fast-charge concept to develop a physics-based approach to battery SOP estimation.

Shortcomings of the bisection method

- The bisection method utilizes a constant-current assumption over the power-prediction interval in its computation of power limit estimates.
- This necessarily gives rise to conservative approximations.
- This is easy to see if we consider how the action of the bisection method appears on a VI diagram, as shown in the figure for the charge case.

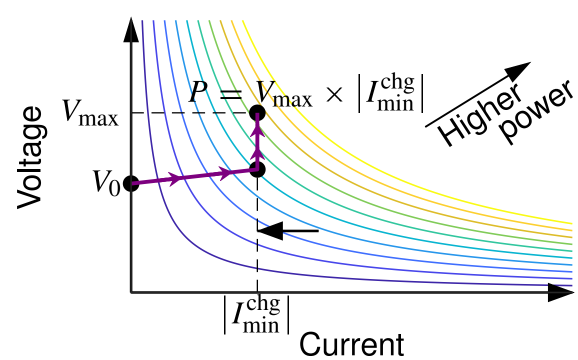

- This figure shows the discharge case.
- Note that the horizontal left-pointing arrows in the figures indicate the value of constant current that the bisection algorithm seeks to optimize.

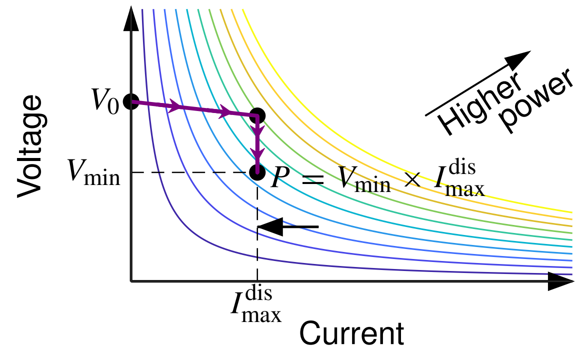

- First, under the assumption of constant current for the duration of ΔT, it is not possible to maintain constant voltage during the same interval simultaneously, meaning that the respective bounds $V_{\min}$ and $V_{\max}$ are enforced only at the end of the power-prediction window.
- Resulting SOP estimate is the power contour level intersected by the trajectory corner point marked $P = V_{\min} \times I^{\text{dis}}_{\max}$ in the discharge figure.
- An alternative method inspired by model predictive control (MPC) instead considers the full dynamic nature of the predicted trajectories.
- We conjecture that by taking account of time-varying predictions throughout the time-horizon interval, a more accurate SOP may be obtained. Next, we present the MPC method of power limit estimation.

Basic idea

- Ch. 7 introduced MPC as a real-time computational control method that can predict dynamic behavior, optimize to a specified performance criterion, and enforce hard constraints.
- There, we applied MPC as a control method to compute an optimal fast-charge profile, while enforcing hard constraints on internal electrochemical variables, thereby eliminating the conservatism inherent using voltage limits alone.

- Inspired by this result, it is natural to ask here whether we can adopt a similar methodology to estimate SOP; and therefore the remainder of this section will endeavor to address this question.
- As with PL-BSM previously, in this approach, we shall compute an estimate of available charge and discharge power over a finite-time power horizon, ΔT.
- The method executes a constrained MPC algorithm at each sample point to predict an optimal future power profile and then numerically integrates time-varying instantaneous power to compute total energy.
- It then averages the total energy over a finite time horizon to provide an estimate of maximum sustainable power.
- It is important to note here that the MPC algorithm is used here not to control the battery, but rather to inform the BMS.
- The PL-BSM approach to power limit estimation, as seen previously, relies on a straight-line prediction of cell dynamics over a finite time horizon, as depicted in the figure.

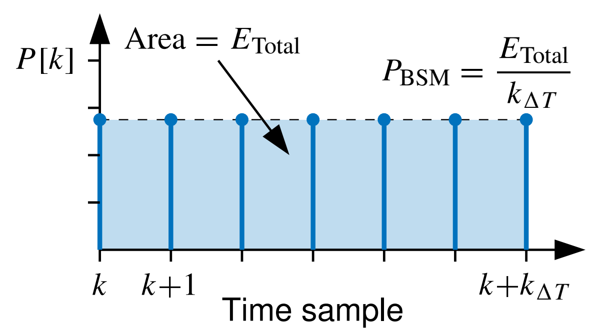

- Here, the dynamic predictor uses the system model to compute the instantaneous power $P[k] = v[k] \times i[k]$ at time value $k + k_{\Delta T}$ such that it adheres to specified voltage (and perhaps other) hard limits.
- This value is then used directly as an estimate of maximum sustainable power.
- In other words, the PL-BSM method considers the area of the shaded rectangle in the figure as the total charge-discharge energy estimate

over the power horizon, and distributes this energy at a constant power level, $P_{\text{BSM}} = {}^{E_{\text{Total}}}/_{k_{\Delta T}}$.

- By contrast, the MPC-inspired method uses a dynamic predictor—together with step-wise constrained optimization—to compute an optimal fast-dis/charge profile that adheres to hard constraints, as shown in the figure.

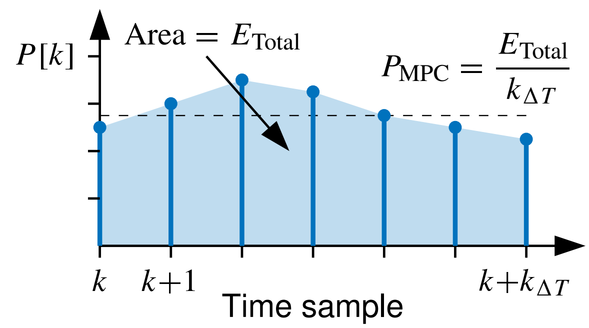

- The optimal profile of instantaneous power values is numerically integrated to obtain a computation of total energy.
- This value reflects the largest amount of energy that can either be inserted or removed from the battery cell over the specified power horizon while respecting constraints.
- Taking the average of this total energy value gives an estimate of the maximum sustainable power than can be inserted/extracted from the battery upon charge/discharge respectively.
- It is interesting to note that in this sense, PL-MPC gives a near-optimal *instantaneous power profile* for the duration of ΔT.
- This means the maximum charge/discharge energy computed can be achieved by following the prescribed current profile.
- It is not, however, a tight bound on the sustainable energy level; this can be seen be seen by examining some simulation results.

Model predictive SOP estimation

- MPC was introduced in Ch. 7 in the context of battery fast-charge.

- SOP estimation will employ precisely the same MPC computation used to solve the pseudo-minimum-time problem for fast charge, only in this case the resulting optimal input values are not implemented for control but are used strictly as input to the SOP estimation procedure.
- The algorithm outlined here executes one optimal constrained MPC calculation at each time instant for which an SOP estimate is desired.
- For consistency with the predictive SOP framework, the prediction horizon index N_p is selected so that the MPC time horizon $N_\mathrm{p} \times T_\mathrm{s}$ is less than the power horizon ΔT.
- Of course, this is not a requirement, but rather a convenient choice that promotes computational efficiency.[5]
- The MPC-based power estimation algorithm is outlined in Algo. 8.1.

Algorithm 8.1 MPC SOP estimation.

- Initialization
  - Define initial augmented state-space model matrices $\widetilde{\boldsymbol{A}}_0,\ \widetilde{\boldsymbol{B}}_0,\ \widetilde{\boldsymbol{C}}$
  - Select MPC tuning parameters: $N_\mathrm{p},\ N_\mathrm{c}$, and ρ
  - Compute corresponding initial MPC prediction matrices, $\Phi_0,\ \boldsymbol{G}_0$
- Power prediction loop
  - For simulation sampling time $k = 1, \ldots,\ N_\mathrm{sim}$:
    - Update time-varying matrices $(\widetilde{\boldsymbol{A}}_k,\ \widetilde{\boldsymbol{B}}_k,\ \Phi_k,\ \boldsymbol{G}_k)$
    - Update constraint bounds via $\boldsymbol{M}_k,\ \gamma_k$
    - Compute optimal input sequence, $\left\{\Delta \underrightarrow{\boldsymbol{u}}[k]\right\}$ which satisfies constrained fast-charge or fast-discharge objective over power horizon
    - Compute instantaneous power as $P[k] = v[k] \times i[k]$, for $k = 1 : k_{\Delta T}$
    - Compute numerical integral of $P[k]$ over the interval $k = 1 : k_{\Delta T}$ to obtain total energy, $E[k]$
    - Compute available power $P_{\mathrm{chg,min}}$ or $P_{\mathrm{dis,max}}$ at sample time k as $\dfrac{E[k]}{(k_{\Delta T} \times T_\mathrm{s})}$
    - Propagate state equations

[5] It is of course possible to design alternative MPC strategies for this computation which use different horizon lengths (e.g., a shrinking horizon). Numerical experiments show some advantages may be gained, but overall, results are similar.

8.6: Examples of model predictive SOP estimation

- We now demonstrate MPC-based SOP estimation by applying both the BSM algorithm and the prior MPC-EKF code to the NMC30 cell.
  - A 9-state HRA-ROM (8 echem. states plus integrator) was used.

Case 1: Establishing a performance baseline

- Case 1 imposes hard limits on applied current and cell voltage.
  - Maximum current is constrained to a magnitude of 150 A (5C) for both charge and discharge.
  - Cell terminal voltage limits were set to $V_{\max} = 4.2$ V and $V_{\min} = 3.3$ V.
- The simulation utilizes a sequence of charge-depleting UDDS profiles applied over a total time of 42 000 s (11.67 h).
- Cell voltage (when no power limits are enforced) is shown to the right.

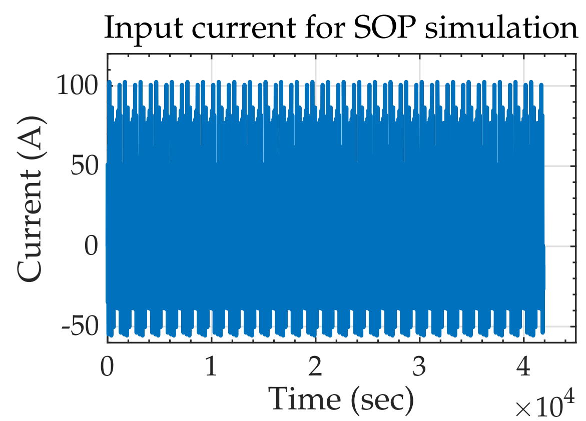

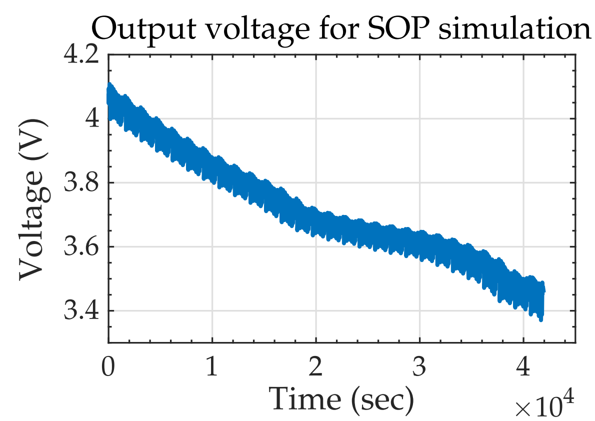

- Figures show SOP estimates for $\Delta T = 10$ s (left) and 20 s (right).

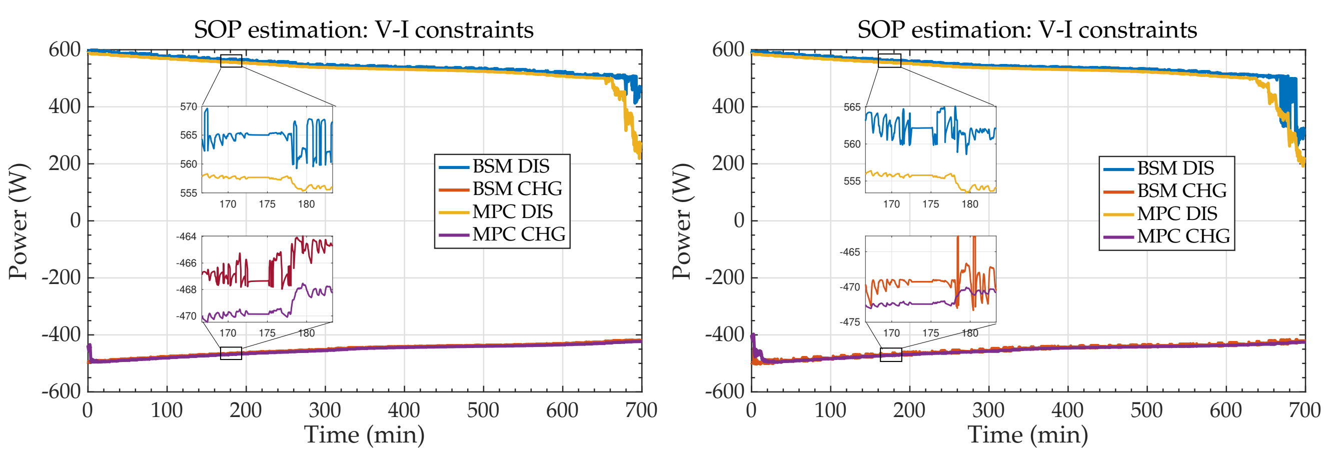

- In order to ensure compact prediction matrices and efficient computation, MPC horizons of $N_\mathrm{p} = 3$ and $N_\mathrm{c} = 2$ were selected.[6]
- As one would expect, available discharge power diminishes with decreasing SOC and terminal voltage.
- Note that power estimates become increasingly erratic at low SOC values where linearized model behavior is generally less accurate.
- Available charge power also exhibits a steady decline aligned with a corresponding decrease in battery voltage levels.
- In this case, the SOP estimate is essentially the product of the maximum applied charge current and the voltage that can be attained over the power horizon from the given operating point with application of constant maximum current.
- It's not too surprising that both BSM and MPC algorithms give very similar results for this particular case, generally agreeing within $1\,\%$ over most of the simulation.
- Computed estimates diverge more significantly at the SOC extremes where BSM tends to overestimate the available power.
- This discrepancy is more apparent at the longer power horizon, where we also can observe a larger decrease in available discharge power as SOC approaches very low values.

Case 2: Placing limits on internal electrochemical variables

- Case 2 demonstrates the viability of using estimates of internal electrochemical states to refine SOP values further.

[6] Numerical experiments indicated only marginal improvements in the SOP estimate were obtained with larger values of these parameters.

- Cell-voltage constraint is removed; replaced with constraints on solid surface conc. ($\theta_{\text{ss}}^{\text{n}}$) for discharge and overpotential ($\phi_{\text{s-e}}^{\text{n}}$) for charge.
  - Both quantities are denoted for the negative electrode.
- Figures show simulation results for BSM and MPC SOP algorithms computed for the same power horizons used in Case 1.

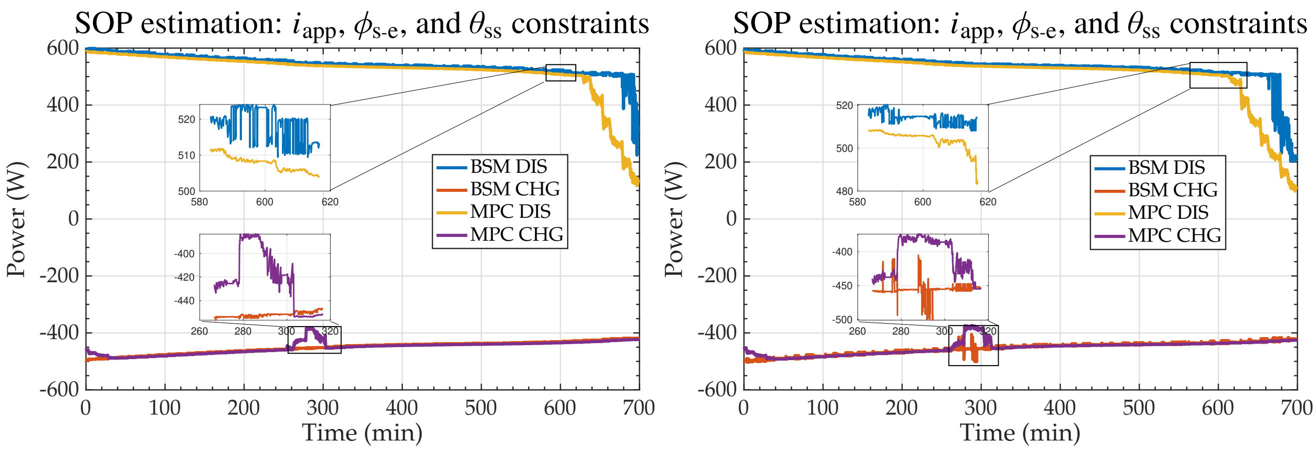

- The available charge power shows some interesting differences from what we observed in the previous case.
  - e.g., starting around 275 min, we note a decrease in charge power.
- This comes about when the algorithm anticipates that overpotential $\phi_{\text{s-e}}$ is about to reach its lower bound, and risk Li plating at the anode.
- As a consequence, allowable current levels are decreased in this operating region thus lowering the available power estimate.
- We further note that the BSM approach struggles to capture this effect correctly since the overpotential value hovers very close to its lower bound.
- MPC, on the other hand, foresees this impending breach before it occurs and takes protective action.

8.7: MATLAB toolbox

- The SOP algorithms featured in this chapter have also been incorporated in the MATLAB toolbox.
- A flow diagram depicting the overall structure of the BSM SOP-estimation method is shown below.

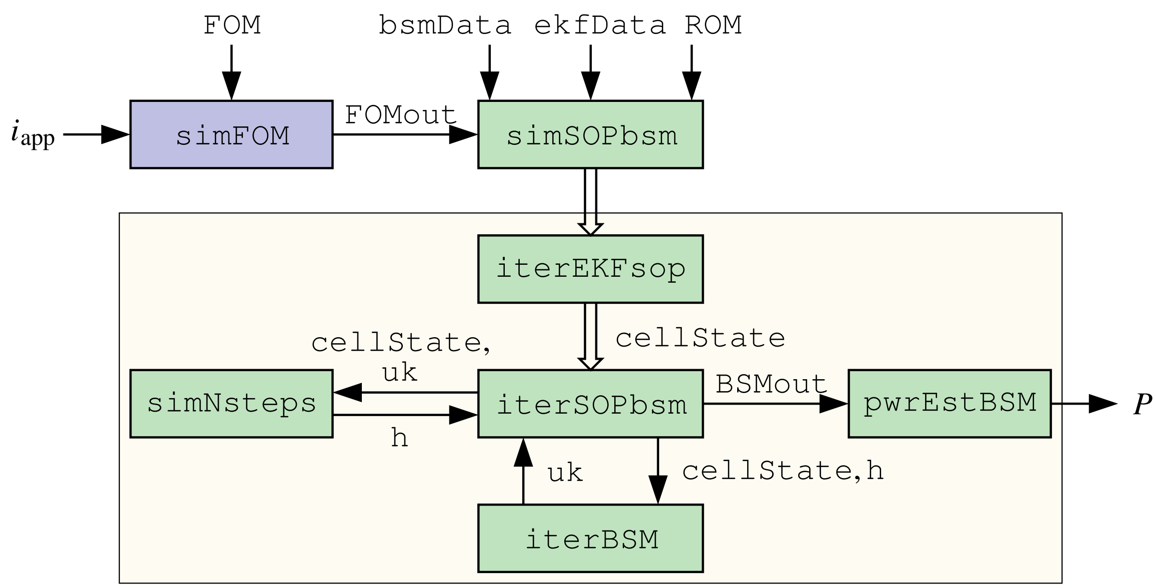

- A flow diagram depicting the overall structure of the MPC SOP-estimation method is shown below.

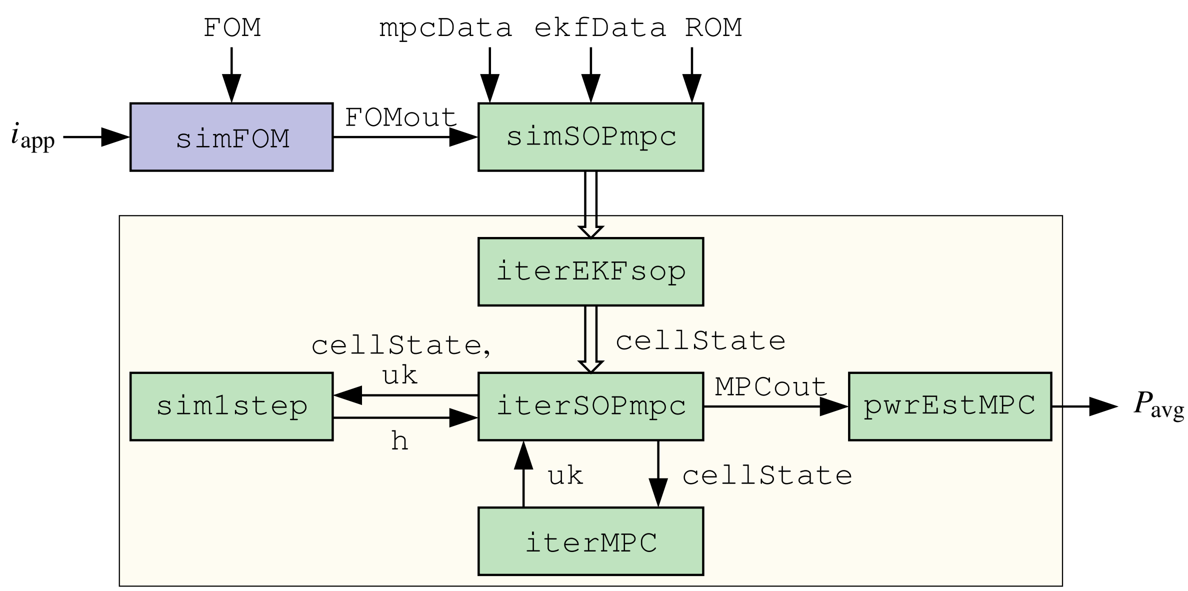

- The first step generates the FOM output for a designated input profile, i_{app}, accomplished here via the FOM simulation block `simFOM`.

- This step can be carried out by any of a number of available numerical simulation packages specialized to full-order battery modeling.
- Output variables contained in `FOMout` then serve as input to the `simSOP[xxx]` routines initiating either BSM or MPC algorithms.
- Note also that `simSOP[xxx]` utilizes data supplied by structures `bsmData`, `ekfData`, as well as the appropriate `ROM`.
- `simSOP[xxx]` orchestrates the remainder of the SOP estimation process by first calling a Kalman filter routine to generate estimates of the cell's internal state and provide updates to the state matrices.
- From this point on, the two methods operate differently, executing the algorithms detailed in the previous sections.
- The main code for `simSOPbsm` is shown for reference:

```
% SIMSOBPBSM:  This function carries out the steps required to implement
%              the bisection method for SOP estimation
% Inputs:
%   bsmData:    data structure containing bisection parameters
%   FOMout:     data structure containing FOM simulation output
%   ekfData:    data structure containing extended Kalman filter output
%   ROM:        data structure defining ROM
% Outputs:
%   SOP_BSMresults_x:   data structure containing BSM SOP results
function [SOP_BSMresults_DIS,SOP_BSMresults_CHG] = simSOPbsm(bsmData,
         FOMout,ekfData,ROM)

  % Set up preliminaries
  Nsim = length(FOMout.Iapp);
  bsmData_DIS = bsmData;
  bsmData_CHG = bsmData;
  initVariables;             % function to initialize data variables

  % Run main program
  for k = 1:Nsim
    vk = FOMout.Vcell(k);    % cell voltage [V]
```

```
    uk = FOMout.Iapp(k);      % applied current [A]
    Tk = FOMout.T(k);         % temperature [C]

    % Run Kalman filter
    [zk,zbk,ekfData,Xind] = iterEKF_SOP(vk,uk,Tk,ekfData);
    zkEst(:,k) = zk; zkBound(:,k) = zbk;
    ekfData.k = k;
    gamma(:,k)=Xind.gamma; theT(:,k)=Xind.theT; theZ(:,k)=Xind.theZ;

    % DISCHARGE CASE
    if zk(end) > bsmData.DISref
      hdk = @(x) iterSOPbisect(x,ROM,ekfData,bsmData_DIS,'DIS');
      [idbk(k) BSMout] = bisect(hdk,0,bsmData.const.u_max,10e-5,k);
      SOP_BSMresults_DIS = storing(BSMout,SOP_BSMresults_DIS,k);
    else
      idbk(k) = 0;
    end
    P_dis(k) = bsmData.const.v_min*idbk(k);

    % CHARGE CASE
    if zk(end) < bsmData.CHGref
      hck = @(x) iterSOPbisect(x,ROM,ekfData,bsmData_CHG,'CHG');
      [icbk(k) BSMout] = bisect(hck,bsmData.const.u_min,0,10e-5,k);
      SOP_BSMresults_CHG = storing(BSMout,SOP_BSMresults_CHG,k);
    else
      icbk(k) = 0;
    end
    P_chg(k) = bsmData.const.v_max*icbk(k);
  end
end
```

Where to from here?

- We have now reached the end of this three-course series on BMS.
  - What an incredible journey!
- In ECE5710, we developed both empirical and physics-based lithium-ion cell models; in ECE5720, we explored BMS algorithms based on empirical ECMs; and finally, in this course, we investigated ways to make BMS algorithms based on PBMs practical.

- To do so, we first had to overcome several roadblocks.
- We discovered that one challenge to using PBMs in a BMS is that not all of the parameters of the DFN model are identifiable.

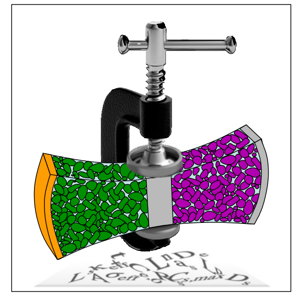

  - So, we applied a parameter-lumping process to the model equations to generate the reformulated LPM.
  - All LPM parameters are identifiable, meaning they can be estimated from current/voltage measurements, in principle.
- We then found that a second impediment to using PBMs is that the DFN model does not describe all experimentally observed cell dynamics.

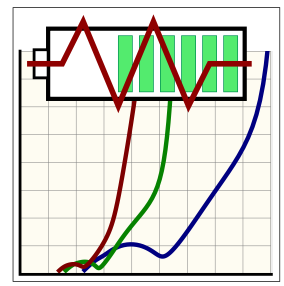

  - So, we enhanced the DFN model by substituting the more general MSMR model for the Butler–Volmer kinetics.
  - We added a description of an electrical double layer to the electrode/electrolyte interface.
  - We generalized the double-layer and solid-diffusion descriptions by incorporating CPEs in the model, and we added a physics-based model of SOC dependence to electrode solid diffusivity.
  - Due to the addition of CPEs, this model can be evaluated in closed form only in the frequency domain (but we learned later how to make a high-fidelity approximation in the time domain).
  - We developed a set of exact closed-form equations (TFs) that allow computing the frequency response of any electrochemical variable at any spatial location in the cell very quickly.

- By combining TFs, we derived a closed-form expression of cell impedance, which can be visualized using Nyquist plots, which are commonly used to display cell impedance measured via EIS.

- A third obstacle to using PBMs in BMS is the need to estimate all cell-model parameter values.
  - We focused on nonteardown approaches to do so.
  - Even though it is mathematically possible to estimate all LPM parameter values from current/voltage data, the sheer number of parameters that must be estimated and the fact that nonlinear optimization is required makes the problem very challenging.
  - We proposed a divide-and-conquer approach that determines subsets of parameter values using targeted laboratory tests.
    - OCP testing allows us to estimate OCP versus stoichiometry for both electrodes (absolute for neg; relative for pos).
    - OCV testing determines the electrode operating boundaries and cell capacity.
    - Discharge testing improves the calibration of the positive-electrode OCP function vs. absolute stoichiometry and makes finding OCP of both electrodes possible without cell teardown.
      - Pulse testing exposes the parameters of the potential and kinetics equations in the LPM.
      - EIS testing enables estimation of most of the remaining parameter values.
      - Finally, discharge testing combined with pseudo-steady-state model allows us to find the last remaining parameter value.

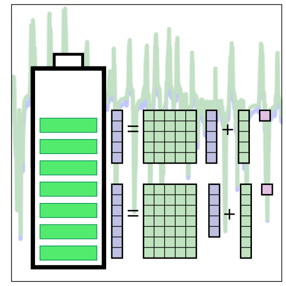

- The fourth challenge to using PBMs in BMS is the fact that they are computationally very intensive.
  - ECE 5710 showed how to use a subspace-projection method—the discrete-time realization algorithm (DRA)—to convert TFs to discrete-time state-space ROMs that can be simulated quickly.
  - This course presented an improved method—the hybrid realization algorithm (HRA)—that performs the same operation much more quickly and requires much less memory.
  - Substeps of the HRA enable validation of the discrete-time frequency response of the ROM versus the original TFs, which gives insight into how well the final model is approximating each of the TFs that it is seeking to reproduce.
  - We also compared the model-blending approach from ECE5710 to a new output-blending approach to using multiple ROMs to provide robust predictions over a wide operational window, and discovered that the output-blending approach is often much better.
  - Finally, we saw ways to use a set of ROMs describing multiple cells having distinct parameter values to simulate battery packs comprising those cells wired in parallel and series.
- Having addressed these fundamental impediments to being able to use physics-based models in a BMS, we began to look at applications of these models to satisfy BMS-algorithm requirements.

- ECE 5720 introduced the nonlinear EKF and SPKF as methods to estimate cell SOC using circuit models.
  - In this course, we discovered that we can also apply EKF and SPKF to estimate the state of a physics-based ROM.
  - But since the ROM describes much more than simply cell SOC or voltage, we can now also estimate any of the electrochemical variables of the cell at any spatial location(s) of interest.
  - To do so, we needed to add a step 3 to the xKF framework, greatly enhancing the predictive capabilities of the methods.
  - We also saw how to apply xKF to an output-blended model, to make accurate state and internal-variables predictions over a wide operational range.

- We explored some concepts in BMS diagnostics and prognostics.
  - We paid special attention to how a cell's OCV relationship changes as the cell ages and how this can give us information regarding the kinds and levels of degradation that are occurring.
  - We discussed some real-time approaches to adapting or selecting a model that best describes the cell under observation at its present point of age.
  - And we presented several thermal and degradation models in lumped-parameter format, for use in power-limits calculations.

- Having developed the tools for lithium-ion battery modeling and state estimation, we next examined some real-time applications of advanced battery management methods.

- To that end, we outlined a fast-charge strategy employing model predictive control to compute an optimal charge current profile that respects hard constraints on problem variables of interest.

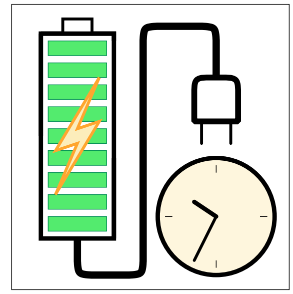

  - Numerical simulations demonstrated the viability of the approach and its potential to extend battery lifetime by mitigating true mechanisms of cell degradation.

- Finally, we examined the important topic of energy management within a battery from the standpoint of a state of power measure.

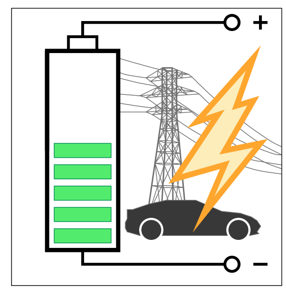

  - In addition to the remaining energy a battery contains, we considered the implications of how quickly that energy is added to or removed from a battery in terms of its power utilization.
  - Such a measure is a governing factor in vehicle performance. Again utilizing and MPC framework, we developed an advanced real-time SOP estimation algorithm and demonstrated its operation via numerical simulation.

- This course has presented our best understanding at this point in time of best practices relating to physics-based modeling of lithium-ion cells and of physics-based BMS algorithms.

- But this field is developing at a rapid pace.

- Our own research team and teams at other universities and research institutes are making steady progress.
- The community has not yet converged on any best modeling methods or practices, or best battery-management approaches.
- We fully expect this field to continue to evolve, driven by the need to support the significant investments in large-scale battery-based installations (and hence the urgency of making them work safely, optimally, and robustly for as long a service life as possible).
- We envision ongoing refinements to the fundamental lithium-ion PDEs, perhaps improving descriptions of cell dynamics at low SOCs, low temperatures, and high C-rates.
  - (We also expect to see the approaches presented in this series start to be applied to other battery types, featuring new anodes such as lithium-metal and silicon, solid electrolytes, and new cathode materials like sulphur.)
- We anticipate advances in nonteardown methods to estimate model parameter values.
  - We are pleased with the OCV and teardown-based OCP estimation methods, but there is considerable room for improvement in nonteardown-based OCP estimation.
  - We know that OCV should equal the positive electrode's OCP minus the negative electrode's OCP, but experimental errors accumulate and there is room for refining these estimates to achieve better agreement at the cell level.

- We have found that the pulse-resistance test provides accurate parameter estimates for some cells but not for others.[7]
- Since the pulse-resistance test is the only one of those that we have presented that is designed to expose the parameters describing the nonlinearities in the cell, different tests must be developed that somehow use a variety of C-rates to actuate the cell in ways that enable estimating these parameter values efficiently and accurately.

■ We have a strong affinity to the HRA ROM, especially for simulations of fresh cells, but we admit that it does have some shortcomings.

- The most limiting of these is that the HRA is a numeric method that obscures the connection between physical parameter values of the PDEs in the final ROMs.
- It is an open problem to determine how to adjust the coefficients of these ROMs in a physically meaningful way as the cells being managed by the BMS age.
- We have presented some of our thoughts on how to approach this problem in this course and even have some preliminary results along these lines, but there remains significant work to do.
- One possibility is to replace the ROM with a single-particle model (SPM) or enhanced single-particle model (SPMe) for some applications; the methods of Chaps. 1 to 3 in this course still apply to that case, but the approaches of Chaps. 4 to 8 would need to be redeveloped for the different model equations of the SPM.

[7] We think that perhaps $\bar{R}_{\mathrm{dl}}$ is too small on some cells for the data quality to be sufficient to find good estimates of the values of the kinetics and potential equations. This might be improved by using larger-magnitude current pulses.

- Research on physics-based fast-charge and state-of-power estimation shows great promise, but is still in its infancy.
  - It remains to perform comprehensive experimental validation of these techniques, which may point the way to further refinements.
- At the time of this writing, other topics worthy of investigation in this rapidly emerging field include new models of lithium plating/stripping, pulse-charging techniques, as well as advances to improve performance/robustness of MPC for nonlinear systems.
- In closing, we hope that this series has been helpful to your understanding of Li-ion battery cells and how they can be managed by a BMS that uses either empirical or physics-based models.
- We entrust the next steps to you to apply these methods, refine them, and even replace them with transformational new approaches.
- Best wishes to you as you do so!

Appendix 8.a: Summary of variables

- E_{Total}, total energy $[J]$.
- $E[k]$, total energy computed at time instant k $[W]$.
- $i[k]$, applied current at time instant k $[A]$.
- $i_{\min}^{\text{chg,volt}}[k]$, constant charge current value that brings voltage to a limit over ΔT $[A]$.
- $i_{\max}^{\text{dis,volt}}[k]$, constant discharge current value that brings voltage to a limit over ΔT $[A]$.
- $I_{\max}$, maximum applied current $[A]$.
- $I_{\min}$, minimum applied current $[A]$.
- $k_{\Delta T}$, integer time index for power horizon (i.e., $\Delta T = k_{\Delta T} \times T_{\text{s}}$).
- $P[k]$, cell power at time instant k $[W]$.
- P_{avg},average power over a defined time interval $[W]$.
- $P_{\text{chg,min}}$, SOP estimate of available charge power $[W]$.
- $P_{\text{dis,max}}$, SOP estimate of available discharge power $[W]$.
- P_{inst}, instantaneous power $[W]$.
- $P_{\max}$, maximum instantaneous power $[W]$.
- T_{s}, sampling interval $[\text{sec}]$.
- $v[k]$, cell terminal voltage at time instant k $[V]$.
- $V_{\max}$, maximum allowable cell voltage $[V]$.
- $V_{\min}$, minimum allowable cell voltage $[V]$.
- ΔT, power horizon $[\text{sec}]$.
- $\underline{\sigma}(\boldsymbol{M})$, minimum singular value of matrix $\boldsymbol{M}$.

Appendix 8.b: Adaptive input weighting

- One challenge associated with implementing the MPC method of SOP estimation regards the selection of the input weighting factor, ρ.
- For a stand-alone optimization problem, there exist ad hoc rules (along with trial and error) that give a suitable value for this factor.
- If chosen too small, overly aggressive input actions may result; too large and the response is often sluggish.
- Furthermore, it has been observed that some values of ρ in constrained quadratic programming problems may lead to slow convergence or worse yet, infeasibility conditions.
- Real-time SOP estimation can encounter a wide range of conditions, presenting different SOP optimization problems at each sample time.
- It is impractical to expect that a single ρ value will satisfy all situations.
- In order to address this difficulty, our method incorporates a simple adaptive input weighting strategy designed to ensure the unconstrained input solution (supplied to the quadratic program) is approximately of the same vector norm as the constraint bound.
  - This is analogous to a "warm start" for the Hildreth algorithm.
  - The conjecture here is that by starting the constrained optimization algorithm close to the constraint boundary, the algorithm will be better behaved and give more consistent constrained solutions.
  - Although we won't prove it, experience shows good agreement with the conjecture. The algorithm is constructed as follows.
- Utilizing the vector-matrix 2-norm we can apply the triangle inequality to express an upper bound on the unconstrained input solution as,

$$\begin{aligned}\left\|\underset{\longrightarrow}{\boldsymbol{\Delta u}}_{k+1}^{*}\right\| &\le \frac{1}{2}\left\|\boldsymbol{H}^{-1}\boldsymbol{g}\right\| \\ &\le \frac{1}{2}\left\|\boldsymbol{H}^{-1}\right\|\left\|\boldsymbol{g}\right\| \\ &\le \frac{1}{2}\left\|\left(\boldsymbol{G}^{T}\boldsymbol{G}+\rho\boldsymbol{I}_{N_{\mathrm{c}}}\right)^{-1}\right\|\left\|\boldsymbol{g}\right\|. \end{aligned} \tag{8.1}$$

- Ideally, we seek a bound on the magnitude of the largest element of the input sequence contained in $\underset{\longrightarrow}{\boldsymbol{\Delta u}}_{k+1}^{*}$, but this is cumbersome.
- Instead, the vector 2-norm gives us a sensible aggregate measure of input size, is relatively easy to compute, and serves as an adequate basis on which to guide the selection of the input weighting value ρ.[8]
- To obtain an absolute magnitude-based algorithm, rewrite Eq. (8.1) by equating the RHS upper bound directly to the constraint value:

$$\left\|\left(\boldsymbol{G}^{T}\boldsymbol{G}+\rho\boldsymbol{I}_{N_{\mathrm{c}}}\right)^{-1}\right\| = \frac{2\Delta u_{\max}\sqrt{N_{\mathrm{c}}}}{\|\boldsymbol{g}\|}$$

where $\Delta u_{\max}$ is the maximum allowable magnitude of the input increment. Rearranging, we have

$$\underline{\sigma}\left(\boldsymbol{G}^{T}\boldsymbol{G}+\rho\boldsymbol{I}_{N_{\mathrm{c}}}\right) = \frac{\|\boldsymbol{g}\|}{2\Delta u_{\max}\sqrt{N_{\mathrm{c}}}}$$

where $\underline{\sigma}(\cdot)$ denotes the minimum singular value.

- Solving for input-weighting factor ρ we obtain the result:

$$\rho = \frac{\|\boldsymbol{g}\|}{2\Delta u_{\max}\sqrt{N_{\mathrm{c}}}} - \underline{\sigma}\left(\boldsymbol{G}^{T}\boldsymbol{G}+\rho\boldsymbol{I}_{N_{\mathrm{c}}}\right).$$

- In practice, ρ is recalculated at each sample point where a constrained solution to the quadratic optimization problem is required within the power prediction loop.

[8] Other norms could be used for computational convenience; one choice is the Frobenius norm—the square root of the sum of the squares of all vector/matrix elements.